LONGSHORE TRANSPORT EVALUATIONS AT A DETACHED BREAKWATER

by

R. O. Bruno[1], R. G. Dean[2], and C. G. Gable[3]

ABSTRACT

A field experiment was conducted by the Coastal Engineering Research Center (CERC) to develop correlations between wave characteristics and longshore sediment transport. The waves were measured by two near-bottom mounted pressure transducers and the average longshore sediment transport rates were determined from sequential volumetric surveys behind an offshore breakwater which was regarded as a total trap. The data analyzed herein encompass a period of nine months during which a total accumulation of 675,000 m^3 occurred as documented by eight surveys. Spectral analyses of the wave data were conducted and yielded one direction per frequency. The correlations include immersed weight sediment transport rate, I, versus (1) longshore component of wave energy flux at breaking, $P_{\ell s}$, and (2) the onshore flux of the longshore component of wave-induced momentum, S_{xy}. The most widely used correlation constant, K, in the relationship $I = KP_{\ell s}$ is 0.77. The best-fit values found from the data were K = 0.65 and 0.92 for linear and log best-fits, respectively, as based on the $P_{\ell s}$ values directed toward the trap. The corresponding values of K_* (dimensional) relating I and S_{xy} are 4.98 m/s and 6.37 m/s, respectively. One feature of this type of trap is the potential for overtrapping if the waves are directed nearly normal to shore.

INTRODUCTION

The need for a quantitative relationship for longshore sediment transport is common to practically all coastal engineering projects. Examples include: channel deepening, design of coastal structures and beach nourishment programs. The most widely used predictor relates longshore sediment transport rate to longshore energy flux at breaking or to some measure of wave-induced momentum flux; these relationships require calibration with field and/or laboratory data. A survey of the available field data demonstrates that of the approximately 56 data points, none are based on both measured wave direction and volumetric accumulations in a total trap. Some are based on visually observed wave directions at a location quite distant from the measured wave heights. In addition, much of the sediment data is based on tracer studies with the attendant uncertainties in estimating depth of effective motion.

[1]Chief, Chesapeake Bay Model Branch, Waterways Experiment Station, Stevensville, MD 21666; Formerly at Coastal Engineering Research Center, Fort Belvoir, VA 22060.

[2]Professor, Department of Civil Engineering and College of Marine Studies, University of Delaware, Newark, DE 19711.

[3]Associate Development Engineer, Scripps Institution of Oceanography, La Jolla, CA 92093; Formerly at Coastal Engineering Research Center, Fort Belvoir, VA 22060.

The present paper describes the analysis of a subset of the measurements carried out at Channel Islands Harbor by the Coastal Engineering Research Center (CERC) during the period 1974 to 1977. The data analyzed herein include wave height and direction measurements as determined from a pair of near-bottom mounted pressure gages located in a water depth of approximately 6 meters. The sediment "trap" is an offshore breakwater in approximately 9 meters of water and the west jetty to the entrance to Channel Islands Harbor, see Figure 1. This "trap" is believed to be nearly complete. The volumetric accumulations over a period of nine months are documented by eight surveys, during which a total sediment volume deposition of 675,000 m^3 occurred. Correlations are presented of longshore sediment transport as inferred from accumulation in the trap with $P_{\ell s}$, the longshore component of energy flux at breaking and S_{xy}, the flux in the onshore direction of the longshore component of momentum.

BACKGROUND

The relationship between immersed weight transport rate of sediment, I, and longshore energy flux at breaking, $P_{\ell s}$, is generally presented in terms of a non-dimensional constant, K

$$I = KP_{\ell s} \tag{1}$$

where for a single wave train of breaking height, H_b, and breaking direction, θ_b, relative to a normal to the beach, $P_{\ell s}$ can be expressed as

$$P_{\ell s} = \frac{\gamma H_b^2}{8} C_{G_b} \sin \theta_b \cos \theta_b \tag{2}$$

in which γ = specific weight of water and C_{G_b} is the wave group speed at breaking. A more useful form of Eq. (1) is obtained by noting that the immersed weight transport rate, I, and bulk longshore sediment transport, Q_s, are related by

$$Q_s = \frac{I}{\rho\left(\frac{\rho_s}{\rho} - 1\right) g \left(1 - p\right)} \tag{3}$$

in which ρ and ρ_s are the mass densities of water and sediment respectively, g is the gravitational constant and p is the in-place porosity of the sediment. Combining Eqs. (1) and (3)

$$Q_s = \frac{K}{\rho\left(\frac{\rho_s}{\rho} - 1\right) g \left(1 - p\right)} P_{\ell s} \tag{4}$$

It is noted that the above equations for longshore sediment transport do not account for sediment size, beach slope, porosity, etc. and thus it is very unlikely that "K" is a true constant; however, the tests conducted to date have not provided the ranges of independent

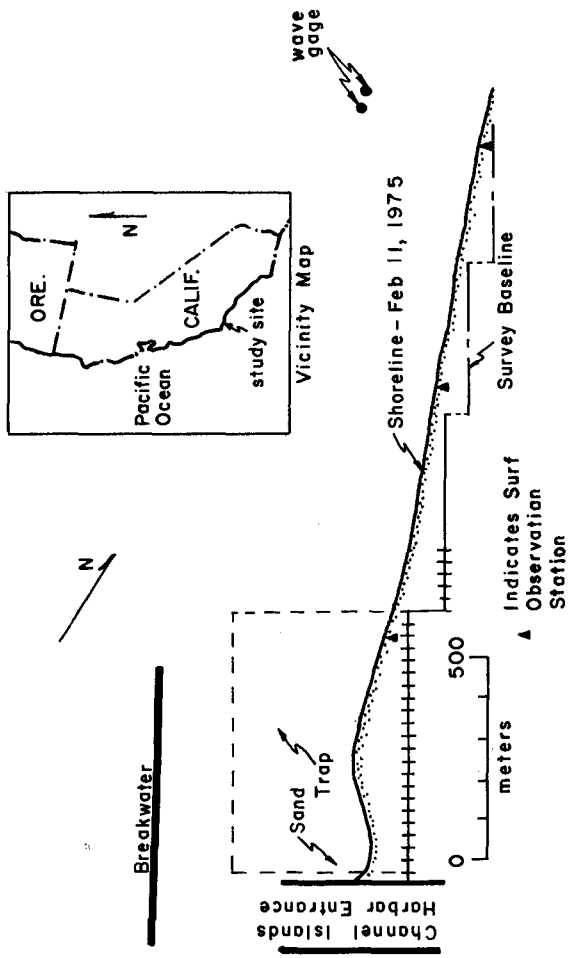

Figure 1. Location Map and Orientation of Field Area.

variables (e.g. sediment size) or accuracy necessary to distinguish the effects of these variables.

A brief review of previous field data is helpful in assessing the currently used relationship. In this review, the laboratory data will be omitted as they do not represent a properly scaled version of the prototype since the scaled sediment size is significantly larger than is usually present with sand-sized particles. The following review is presented in chronological order of the various investigations which have yielded the data. Other reviews have been presented by Das (1971, 1972) and Greer and Madsen (1978).

South Lake Worth Inlet, FL (Watts, 1953)

Longshore transport rates were based on quantities of sand transferred by a permanent sand bypassing plant on the north jetty of South Lake Worth Inlet. The pressure drop of the bypassing pump was correlated with sand discharge by a series of pumping events into a diked disposal area on the downdrift (south) side of the inlet and subsequent surveys of the associated volumes. Thereafter transport rates were inferred from the (calibrated) pressure drop of the pump. The wave characteristics were based on: (a) wave height measurements from a staff gage mounted on the South Lake Worth pier some 16 km north of the inlet, and (b) visual observations of wave direction at the surf line as obtained from a vantage point approximately 6 km north of the inlet. This study yielded four data points with a sediment diameter of approximately 0.4 mm. The average K value is 0.90 with a standard deviation of 0.11.

Anaheim Bay, CA (Caldwell, 1956)

Dredge material from the entrance to Anaheim Bay was placed on the downdrift (southeast) shore and repeated surveys of this area were conducted as the material was transported in a southerly direction. The changes in volume were interpreted as longshore transport rates and the estimates of longshore component of wave energy flux were based on (a) wave staff measurements from the Huntington Beach Pier, some 9 km to the south, and (b) wave directions based on hindcasts and recognition of the sheltering by the offshore islands for waves originating from certain directions. This study provided a total of five data points with a sediment diameter of approximately 0.40 mm. The average K value is 0.76 and the standard deviation is 0.38.

Cape Thompson, AK (Moore and Cole, 1960)

The growth of a spit and the associated waves were observed over a three-hour period. The spit volumes were measured by plane table survey and wave characteristics were based on visual estimates. Only one data point was obtained with a K value of 0.25 for a sediment size of 1.00 mm.

Santa Barbara, CA (Johnson, 1952 and Galvin, 1969)

These data are based on two separate sources. The volumetric data were developed by Johnson (1952) from spit accumulations in the shelter

of the terminus of the Santa Barbara breakwater. The longshore energy values were developed by Galvin (1969) and represent a combination of hindcast wave heights and wave directions selected to result in the maximum longshore energy flux and still be realistic. This data set includes a total of five points with average and standard deviation values for K of 1.60 and 0.70. The sediment size was approximately 0.20 mm.

Silver Strand, CA and El Moreno, Baja California (Komar and Inman, 1970)

These data represent transport over fairly short time intervals as determined from sand tracer measurements and wave energy fluxes derived from an array of wave sensors. Sand transport volumes were usually determined over a fraction of a tidal cycle as the product of the width of the surf zone, the longshore displacement of the center of gravity of the tracer and the thickness of tracer movement. The latter quantity was based on observations of the depth to which a cylindrical "plug" of tracer had been eroded over the observational period and depth of tracer in cores. Values of this depth ranged between 2 and 10.5 cm. These measurements yielded a total of 14 data points and the average and standard deviation values of K for Silver Strand (four data points) where the average sediment size was 0.18 mm are 0.77 and 0.18, respectively. These quantities for El Moreno (10 data points) where the average sediment size was 0.60 mm are 0.82 and 0.27, respectively.

Fernandina Beach, FL (Thornton, 1969)

Mechanical sand traps were placed at discrete locations across the surf zone and used to trap the lower 20 cm of the water column down to and including material in transit on the sand bed. The traps, which were operated from a pier, could be closed and the trapped material pumped up to the pier for measurement. Wave data (height and direction) were based on two wave gages located at the end of the pier. These studies yielded a total of 14 data points with average and standard deviation values for K of 0.048 and 0.027, respectively. The sediment diameter was approximately 0.20 mm.

Channel Islands Harbor, CA (Bruno and Gable, 1976)

These data were based on the same general field program that is the subject of the present paper. The sediment transport rates were inferred from volumetric accumulations behind the Channel Islands Harbor offshore breakwater and the longshore energy flux values were based on Littoral Environmental Observations (LEO). A total of 13 data points resulted with average and standard deviation K values of 1.61 and 1.19, respectively. The sediment size at this site is approximately 0.2 mm.

Discussion

The results presented above comprise a total of 56 data points which are summarized in Table I and presented in Figure 2. It is noted that the Thornton data are significantly lower than the rest and presumably the traps were not effective in collecting the entire sediment transport. Figure 3 represents an attempt to discern any effect of sediment size, D, on the quantity K. If the Thornton data are not con-

TABLE I

SUMMARY OF FIELD DATA AVAILABLE FOR LONGSHORE TRANSPORT CORRELATION AND CHARACTERISTICS OF RESULTING "K" FACTOR

Investigator	Location	Sediment Diameter (mm)	No. of Points	Methods			Characteristics of K		
				Transport	Waves				
					Height	Direction	$\bar{K}$	σ_K	$\frac{\sigma_K}{\bar{K}} \times 100\%$
Watts (1953)	South Lake Worth Inlet, FL	0.40	4	Calibrated Bypassing Pump	M	O	0.90	0.11	19%
Caldwell (1956)	Anaheim, CA	0.40	5	Surveys	M & H	H	0.76	0.38	50%
Moore & Cole (1960)	Cape Thompson, AK	1.00	1	Measured Spit Growth	O	O	0.25	--	-
Johnson (1952) & Galvin (1969)	Santa Barbara, CA	0.20	5	Surveys	H	Max.	1.61	0.70	44%
Komar & Inman (1969)	Silver Strand, CA	0.18	4	Tracers	M	M	0.77	0.18	23%
Komar & Inman (1969)	El Moreno Baja California	0.60	10	Tracers	M	M	0.82	0.27	33%
Thornton (1969)	Fernandina Beach, FL	0.20	14	Bed Load Traps	M	M	0.048	0.027	56%
Bruno & Gable (1966)	Channel Islands Harbor, CA	0.20	13	Offshore Breakwater Trap	O	O	1.61	1.19	74%

KEY

1. M = Measured, O = Observed, H = Hindcast, Max. = Direction Selected to be Realistic and Yield Maximum Possible Transport.

2. $I = KP_{\ell s}$, I = Immersed Weight Transport Rate, $P_{\ell s}$ = Longshore Energy Flux of Waves.

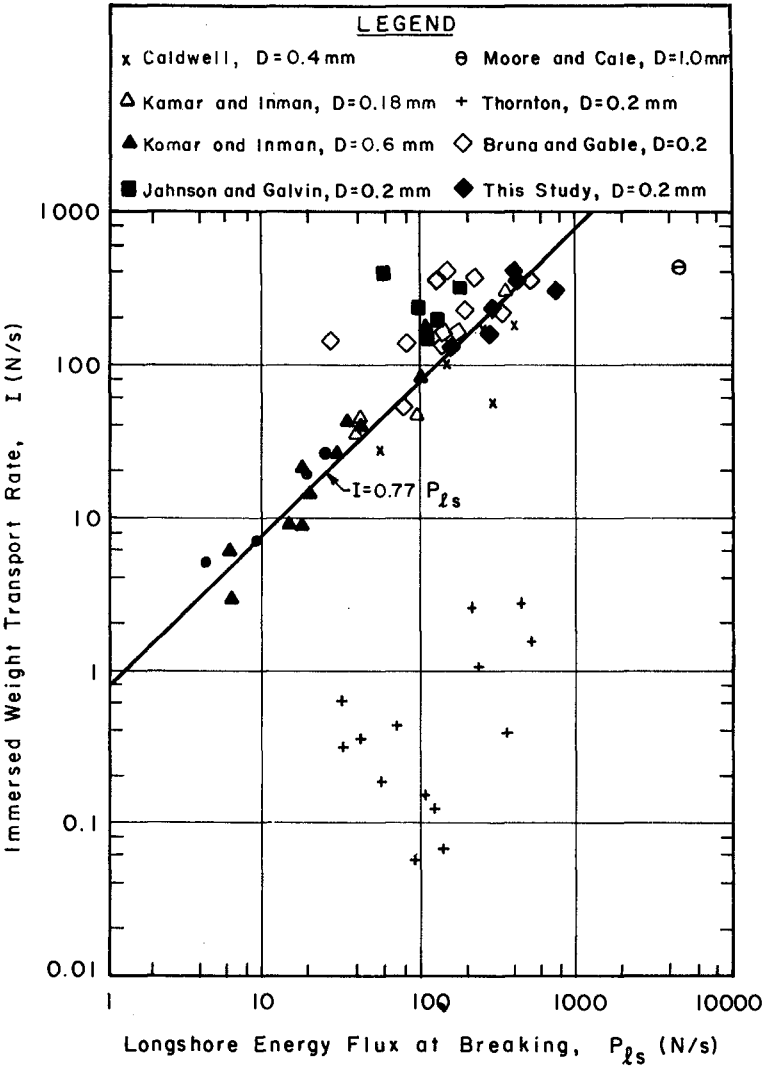

Figure 2, Summary of Field Data I vs. $P_{\ell s}$, Including Results of This Study.

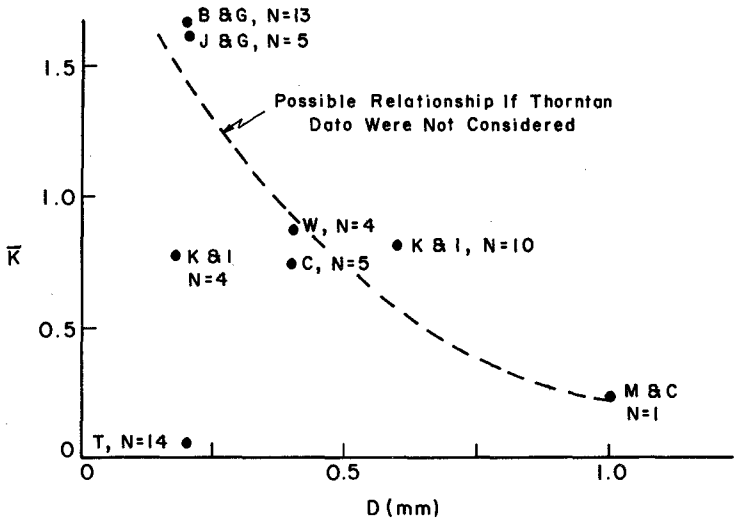

Figure 3. Plot of $\bar{K}$ Versus Diameter, D. Initials and Numbers, N, Refer to Investigators' and Number of Data Points Comprising $\bar{K}$.

sidered, there is a fairly reasonable relationship of increasing K with decreasing sediment size, although there is only one data point for a sediment size exceeding 0.6 mm.

None of the studies of longshore sediment transport have attempted to present an error analysis of the results. Based on the normalized standard deviations (Table I), the results appear reasonably consistent within each data set, yet there is an enormous difference between the average K values of the various data sets, ranging from 0.05 for the Thornton data to 1.61 for the Bruno and Gable data. This would appear to be indicative of large biases in some of the measurements.

In general, it appears that none of the data sets were developed such that high confidence should be associated with both the wave and sediment volume data. In those studies for which the volumetric data were well-established, the wave data usually included one or more visually estimated wave parameters (height and/or direction). In the reported tracer studies, it is believed that the inferred sediment transport rates represent an overestimate of the actual transport. This expected bias is due to the estimate of the shore-parallel displacement of the center of gravity of tracer displacement being obtained from the upper 5 cm of the sediment column since a shear transport must exist within the sand bed with the upper layers moving most rapidly. Additionally, the use of a single value of thickness of transport based on the depth of erosion of a tracer plug should lead to an upward bias as the maximum erosion depth is expected to increase with time. Finally,

the longshore sediment transport in the surf zone is expected to be both spatially and temporally variable although these scales are presently unknown. Since the tracer studies represent longshore sediment transport over only a portion of a tidal cycle, it is surprising that they do not exhibit greater scatter, i.e. percentage standard deviations of 23% and 33% for the Silver Strand and El Moreno K values respectively. One of the advantages of a relatively long-term, complete sediment trap is that it integrates the temporal and spatial variability, thereby providing a good basis for investigating the mean structure of the transport phenomenon before attempting to measure and understand the fine structure.

The complexity of longshore sediment transport, the uncertainties and differences exhibited in the available data and the economic and functional impact of a valid quantitative predictor of transport certainly justify substantial future field and laboratory investigations.

SITE CHARACTERISTICS

Channel Islands Harbor (CIH) is located some 80 km northwest of Los Angeles, CA. The sediment trap is formed by an offshore breakwater parallel to the shoreline and the western jetty of the entrance to Channel Islands Harbor, see Figure 1. The offshore breakwater is some 700 m in length, is approximately 400 m offshore and is in a water depth of 9 m. The entrance to CIH was dredged in 1960-1961 and since that time the material impounded in the sediment trap has averaged approximately 1,000,000 m^3/year. The capacity of the trap is approximately 2,000,000 m^3 and usually the material is pumped (on a biennial basis) a distance of some two kilometers to the downdrift side of the entrance to Port Hueneme, CA, although material is occasionally placed in the "pocket beach" formed by the eastern jetty to CIH and the western jetty to the Port Hueneme entrance approximately 1.6 km to the east. An excellent description of the general characteristics of the site is presented by Herron and Harris (1966).

Although the net sediment transport is from northwest to southeast, periods of reversal do occur. The average sediment size at the site is approximately 0.20 mm; the textural characteristics of the material deposited in the trap have been reported by Bruno, Watts and Gable (1977).

One feature of an offshore breakwater is that it will tend to cause an "overtrapping" of material especially during times when the waves approach in a direction nearly perpendicular to the shoreline. This effect can be demonstrated by noting that even for waves propagating directly toward shore, the effects of diffraction will cause deposition in the form of a salient or tombolo behind the breakwater. If this deposited material is removed such that it no longer represents an equilibrium topography, more material will be transported behind the breakwater, etc. Unfortunately, the degree of overtrapping for different wave characteristics is, at present, unknown. A related question arises whether the impounded volumes should be correlated with the net or downdrift component of longshore energy flux. This will be discussed further in the "Analysis" section.

MEASUREMENT PROGRAM

The entire measurement program extended from April 17, 1974 to August 30, 1977. The portion of this program which will be presented in this paper corresponds to the period when two submerged pressure gages were operational and spans the period July 30, 1974 to May 6, 1975.

Wave Measurements

Two total pressure sensors were located near the bottom in a water depth of approximately 6 m. The gages were separated by approximately 23 meters; the geometric characteristics of the gage installations are presented in Figure 4. Pressure records were recorded in digital form approximately every two hours. The records contained 4096 data points at 0.25 sec. each resulting in a record length of 17.07 minutes. The procedure utilized in analyzing the wave records will be presented in a later section.

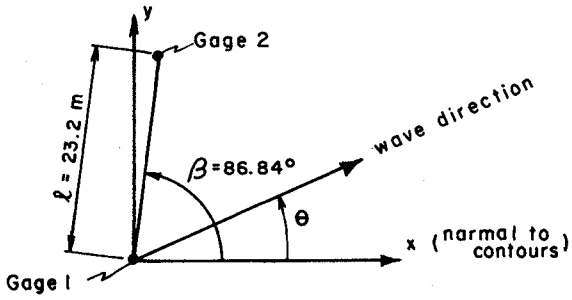

Figure 4. Characteristics of Two-Gage Array at Channel Islands Harbor, CA.

Sediment Volumes

A total of eight surveys were carried out during the period encompassed in this paper. Precision range-range equipment provided horizontal positioning and a standard fathometer was used to establish depths greater than could be obtained by shore-based leveling. The surveys were carried out using a LARC amphibious vehicle, thereby allowing a continuous profile to be obtained from the seaward limit of interest up onto the dry beach. When in water too shallow for the fathometer, a standard surveying rod was held over the side of the LARC and sighted on by a level from shore. This procedure ensured continuity over the entire profile.

The trap extended from the west jetty of the entrance to Channel Islands Harbor to a location 90 meters updrift of the western tip of the

offshore breakwater. In a shore perpendicular direction, the trap extended from the baseline landward of any wave activity, offshore to a distance of 425 meters. Within the trap area, the spacing of survey lines was 30.5 m and further updrift than 250 m from the updrift end of the offshore breakwater, the spacing was increased to 122 m.

ANALYSIS

As noted previously, the wave data consisted of simultaneous records of digitized pressure data from the two sensors located in approximately 6 m of water. In order to calculate $P_{\ell s}$ and S_{xy} at breaking, the following steps were carried out: (1) Calculation of the frequency-by-frequency wave direction and energy at the location of the wave gages; (2) Transformation of the wave spectrum to the breaker line, including shoaling and refraction effects, and (3) Computation of $P_{\ell s}$ and S_{xy} at the surf line. Each of these is described below.

Calculation of Wave Characteristics at Wave Gages

Each of the pressure records consisted of 4096 data points with a time increment of 0.25 sec. The time series were analyzed using a standard Fast Fourier Transform (FFT) program to determine the coefficients. For example, for the pressure time series from Gage 1

$$p_1(t_j) = \sum_{n=0}^{N-1} [a_1(n) - ib_1(n)]e^{\frac{i2\pi nj}{N}} \tag{5}$$

in which $i = \sqrt{-1}$, and N is the total number of data points (= 4096) for each gage.

The FFT coefficients are defined in terms of the pressure time series as

$$a_1(n) - ib_1(n) = \frac{1}{N} \sum_{j=1}^{N} p_1(t_j)e^{-\frac{i2\pi nj}{N}} \tag{6}$$

and the $a_1(0)$ term represents the mean of the record. In calculating the FFT coefficients, there is a large number of "windows" or "tapers" that may be employed in an attempt to reduce the adverse effects of spectral leakage which arises due to representing an aperiodic time series by a periodic series (Harris, 1976). These tapers all have the form

$$p'(t_j) = w(j)p(t_j) \tag{7}$$

in which $p(t_j)$ is the measured pressure and $w(j)$ is a weighting factor. A characteristic of these tapers is that they are unity at the midpoint of the time series and decrease to a lesser value near the two ends. In the present analysis, through a number of test calculations, it was determined that although the effect of tapering at an individual frequency could be substantial, the overall effect on $P_{\ell s}$ and S_{xy} was quite small, generally less than 4%. Thus in the present analysis, no taper was employed.

The depth of water, Δh, overlying the pressure sensors is obtained from $a_1(0)$ and $a_2(0)$ as

$$\Delta h = \frac{0.5}{\gamma} [a_1(0) + a_2(0)] \tag{8}$$

in which γ is the specific weight of seawater. The total water depth, h, is the sum of Δh and the distance, S_G, of the pressure sensors above the bottom (0.3 m).

Each FFT pressure coefficient is transformed to a water surface displacement coefficient by the following linear wave theory relationship

$$\{a_\eta(n), b_\eta(n)\} = \frac{1}{\gamma K_p(n)} \{a_p(n), b_p(n)\} \tag{9}$$

in which $K_p(n)$ is

$$K_p(n) = \frac{\cosh k_n(S_G)}{\cosh k_n h} \tag{10}$$

In Eq. (10) k_n is the wave number associated with the angular frequency, σ_n as obtained from the linear wave theory dispersion relationship

$$\sigma_n^2 = gk_n \tanh k_n h \tag{11}$$

One of the disadvantages of measuring waves with near-bottom pressure sensors is evident by examining Eqs. (9) and (10). For the higher frequencies (shorter wave periods) K_p is very small resulting in very small pressure fluctuations near the seafloor for the higher frequency waves. Thus, to avoid contaminating the calculated water surface displacement, η, it is usually necessary to apply a high frequency cutoff, above which the pressure contributions are discarded. The proper selection of this high frequency cutoff depends on the signal to noise characteristics of the pressure sensor and signal conditioning system. For purposes of the present analysis, the high frequency cutoff was established at a wave period of 3.1 seconds. For a nominal water depth of 6 meters, and a height of the pressure sensor above the bottom of 0.3 m, the pressure signal is attenuated to approximately 16% of its surface value. In the area of interest, where reasonably long Pacific swell occur, it is probably justified to neglect wave energy for periods shorter than approximately 3 seconds.

Denoting hereafter the FFT coefficients for the water surface displacement as a(n) and b(n), it is noted that the coefficients have the following properties

$$\overline{\eta^2} = \sum_{n=1}^{N-1} [a^2(n) + b^2(n)] \tag{12}$$

$$\left.\begin{aligned} a_{\frac{N}{2}+k} &= a_{\frac{N}{2}-k} \\ b_{\frac{N}{2}+k} &= -b_{\frac{N}{2}-k} \end{aligned}\right\} \tag{13}$$

and thus

$$\overline{\eta^2} = 2 \sum_{n=1}^{N/2} [a^2(n) + b^2(n)] \tag{14}$$

Thus the total (kinetic plus potential) energy, E(n), associated with a particular frequency component, n, is

$$E(n) = 2\gamma[a^2(n) + b^2(n)] \tag{15}$$

Wave Direction - Consider the definition sketch in Figure 5 and the following representation for $\eta(x,y,t_j)$

$$\begin{aligned} \eta(x,y,t_j) &= \sum_{n=1}^{N} d(n) e^{\frac{i2\pi nj}{N}} e^{-i(k_x(n)\cos\theta(n) + k_y(n)\sin\theta(n) - \varepsilon(n))} \\ &= \sum_{n=1}^{N} [a(n) - ib(n)] e^{\frac{i2\pi nj}{N}} \end{aligned} \tag{16}$$

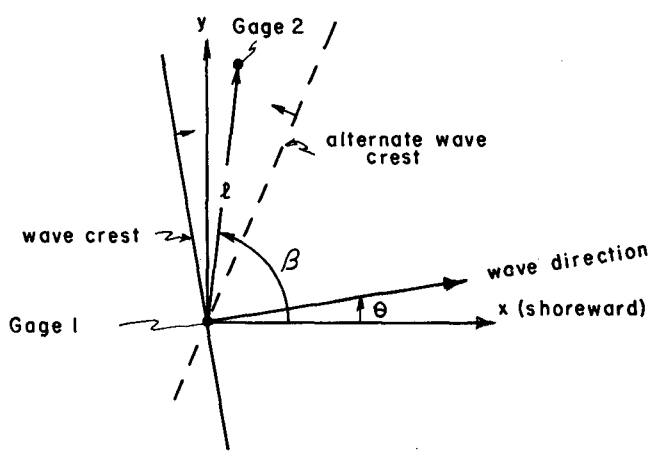

Figure 5. Showing Two-Gage Array Notation and Directional Ambiguity.

Denoting the water surface displacements at the two gage locations as $\eta(x_1,y_1,t)$ and $\eta(x_2,y_2,t)$ and calculating the cross-spectrum, $S_{12}(n)$,

$$S_{12}(n) = \overline{[a_1(n) - ib_1(n)]}[a_2(n) - ib_2(n)] \tag{17}$$

where the overbar denotes the complex conjugate,

$$S_{12}(n) = [a_1(n)a_2(n) + b_1(n)b_2(n)] - i[a_2(n)b_1(n) - a_1(n)b_2(n)]$$

$$= c_{12}(n) - iq_{12}(n) \tag{18}$$

and $c_{12}(n)$ and $q_{12}(n)$ are the "co-spectrum" and "quad-spectrum", respectively of η_1 and η_2. $S_{12}(n)$ can also be expressed as

$$S_{12}(n) = d^2(n)e^{-i[k(x_2 - x_1)\cos\Theta(n) + k(y_2 - y_1)\sin\Theta(n)]} \tag{19}$$

and noting from Figure 5 that the separation distance and orientation of a line joining the two gages are denoted by ℓ and β, respectively, $S_{12}(n)$ can be written as

$$S_{12}(n) = d^2(n)e^{-ik_n\ell\cos(\Theta(n) - \beta)} \tag{20}$$

$$= d^2(n)\cos[k_n\ell\cos(\Theta(n) - \beta)] - id^2(n)\sin[k_n\ell\cos(\Theta(n) - \beta)]$$

Comparing Eqs. (18) and (20), it is apparent that the wave direction, $\Theta(n)$, relative to the x-axis can be expressed as

$$\Theta(n) = \beta \pm \cos^{-1}\left\{\frac{1}{k_n\ell}\tan^{-1}\left[\frac{q_{12}(n)}{c_{12}(n)}\right]\right\} \tag{21}$$

where the ± is the result of a directional ambiguity associated with a two-gage array (Figure 5) and is avoided by choosing the minus sign which selects the wave arriving from the seaward half-plane adjacent to a line joining the two gages.

There are two conditions for which it was not possible to calculate the wave directions $\Theta(n)$. These include poorly conditioned wave data, presumably due to spectral leakage, and spatial aliasing due to the fairly large separation distance (≈ 23 m) between the two gages. If the data are poorly conditioned for determining wave direction, the absolute value of the quantity within the brackets { } in Eq. (21) may exceed unity, clearly a physically impossible condition since the extreme values of the cosine function are ±1. This tended to occur for very long waves for which the energy was small and the value of k_n was also small. The percentage of energy within an individual record for which this condition occurred was relatively small, averaging 2% to 3% with a maximum of approximately 10%. The second condition is related to spatial aliasing

and requires that the wavelength be equal to or greater than twice the projection of the wave gage separation distance in the direction of wave propagation. Referring to Figure 5

$$L > 2\ell[\cos(\theta - \beta)]_{max} \tag{22}$$

which indicates that for the least adverse effects of spatial aliasing, the gages should be on an alignment parallel to the dominant orientation of the wave crests. In our case $\beta = 86.8°$ and in general, the waves approach within approximately 40° of the shoreline. For purposes here, a variable aliasing frequency limit was developed for each record depending on the wave directions for the lower frequencies. Three frequency limits were considered, corresponding to $|\theta - \beta|$ values of 45°, 60° and 75°, with the 75° value associated with the highest frequency limit. Selection of the frequency limit required that 90% of the wave energy in a frequency range $\sigma_A/2$ to σ_A lie within the associated wave direction range, where σ_A is the frequency corresponding to the particular aliasing wave direction (Eq. (22)). For the water depth at the site, the three directional limits of 45°, 60° and 75° are associated with approximate wave periods of 5.3, 4.2 and 3.1 seconds, respectively. The percentage of energy associated with periods shorter than 5.3 s. was substantial in our data, amounting to 25-30%. In later calculations of $P_{\ell s}$ and S_{xy}, an attempt was made to account for the energy above the aliasing frequency by augmenting the calculated values, illustrated for $P_{\ell s}$ as follows, by

$$\left(P_{\ell s}\right)_{cm} = \left(P_{\ell s}\right)_c \frac{E_{TOT}}{E} \tag{23}$$

in which the subscripts "c" and "cm" indicate calculated and calculated modified respectively. E_{TOT} and E represent the total wave energy values and the energy below the spatial aliasing frequency. In a sense, this modification is equivalent to associating the effective direction as determined from the frequencies not affected by the aliasing consideration or poorly conditioned data to all the wave energy.

Transformation of Wave Spectrum to Breaker Line

Determination of Breaking Depth - At this stage, the wave energy and wave direction in the vicinity of the gages are determined. These values are then transformed to the breaker line accounting for shoaling and refraction.

To determine a breaking depth, a method suggested by T. L. Walton was employed in which the total onshore flux of wave energy was equated at the gages and at the breaker line with the requirement that the root-mean-square breaking wave height H_{rms} be related to the water depth by

$$\left(H_{rms}\right)_b = \kappa h_b \tag{24}$$

in which κ was taken as the usual spilling breaker value of 0.78. The total onshore energy flux, F_R, at the reference (gage) location is

$$F_R = 2\gamma \sum_{n=1}^{N/2} [a^2(n) + b^2(n)] C_{G_n} \cos \theta_n \tag{25}$$

in which the subscript "R" denotes the reference location. Considering shallow water conditions for breaking $C_{G_n} = C_G = \sqrt{gh_b}$ and $\cos \theta_b \approx 1.0$, the onshore energy flux at breaking is

$$F_b = \frac{\gamma H_b^2}{8} \sqrt{gh_b} = \frac{\gamma \kappa^2}{8} \sqrt{g}\, h_b^{2.5} \tag{26}$$

Equating F_R and F_b

$$h_b = \left[\frac{16 \sum_{n=1}^{N/2} [a^2(n) + b^2(n)] C_{G_n} \cos \theta_n}{\kappa^2 \sqrt{g}} \right]^{0.4} \tag{27}$$

It is worthwhile to note that neglecting wave refraction in the breaking depth determination does not result in very large errors. For example for a wave direction at the gages of 30°, the error in breaking depth would be less than 6%. For a more realistic overall wave direction of 20°, the associated error in breaking depth is less than 3%.

Transformation of Wave Components to Shore - With the breaking depth known, each wave component is transformed to shore accounting for both wave refraction and shoaling based on linear wave theory.

Wave refraction was computed in accordance with Snell's Law and the assumption that straight and parallel contours existed between the gage and breaking locations,

$$\theta_b(n) = \sin^{-1} \left[\frac{C_b(n)}{C_R(n)} \sin \theta_R(n) \right] \tag{28}$$

Shoaling was based on linear theory, resulting in the value of the sums of the squared FFT coefficients at the breaker line of

$$[a^2(n) + b^2(n)]_b = \frac{\cos \theta_R(n)}{\cos \theta_b(n)} \frac{(C_G(n))_R}{(C_G(n))_b} [a^2(n) + b^2(n)]_R \tag{29}$$

in which the first and second ratios on the right-hand side of the equation represent the effects of refraction and shoaling, respectively.

Computation of $P_{\ell s}$ and S_{xy} at the Surf Line

With the wave energy and direction known at the breaker line, the values of longshore component of wave energy flux, $P_{\ell s}$, and flux in the onshore direction of the longshore component of momentum, S_{xy}, are readily determined.

$$P_{\ell s} = G\left\{2\gamma \sum_{n=1}^{N/2} [a^2(n) + b^2(n)]_b \left(C_G(n)\right)_b (\cos\Theta(n) \cdot \sin\Theta(n))_b\right\} \quad (30)$$

$$S_{xy} = G\left\{2\gamma \sum_{n=1}^{N/2} [a^2(n) + b^2(n)]_b \left(\frac{C_G(n)}{C(n)}\right)_b (\cos\Theta(n) \sin\Theta(n))_b\right\} \quad (31)$$

where the factor G is given by the ratio

$$G = \frac{E_{TOT}}{E} \quad (32)$$

as defined in and discussed in relation to Eq. (23).

It is worthwhile to comment on possible errors due to determination of the breaking depth, h_b. Under the condition of straight and parallel bottom contours as considered here, the value of S_{xy} at the gage and breaker line locations are identical. Since S_{xy} is independent of depth there is no associated error in this estimate and comparison of Eqs. (30) and (31) shows that $P_{\ell s}$ and S_{xy} differ only by the celerity, C_b, at the breaking depth. It follows that if breaking occurs under shallow water conditions (generally a good assumption), the associated error in $P_{\ell s}$ is proportional to the square root of the ratio of the respective water depths. For example, if the breaking water depth is overestimated by 20%, then the associated $P_{\ell s}$ value would be too large by 9.5%.

Determination of Gage and Shoreline Orientations

In the calculation of directional wave properties relative to the shoreline, it is extremely important to establish the orientation of the wave gage array and a representative shoreline orientation.

Orientation of Wave Gages - During the original study, the locations of the wave gages had been established by measuring angles with transits from two known shore stations on the project baseline. These angles were then translated into gage locations through standard geometric procedures. Two sets of such measurements had been carried out on June 24 and 26, 1974. The resulting gage characteristics are presented in Table II.

Although the gage separation distances as obtained from the two surveys differ somewhat more than desired, it is the gage orientations differing by 3.6° that is of particular concern. Thus on June 7, 1980, these variables were reestablished using range-range microwave equipment. Measurements were obtained from three combinations of shore-based locations, thus allowing a much better determination of gage orientation. These results are also presented in Table II and the averages of all values were adopted for purposes of this study.

TABLE II

GEOMETRIC CHARACTERISTICS OF TWO-GAGE ARRAY

Date	Gage Separation Distance	Gage Orientation With Respect to Baseline
June 24, 1974	23.55 m	10.81°
June 26, 1974	22.71 m	14.44°
June 7, 1980		
Trial 1	23.8 m	15.81°
Trial 2	23.2 m	12.74°
Trial 3	22.6 m	12.36°
Values Adopted For This Study	23.2 m	13.23°

Effective Shoreline Orientation - The determination of effective shoreline orientation proved to be a somewhat more difficult problem at this site than originally anticipated. One difficulty is that dredging and subsequent filling by longshore sediment transport in the impoundment area caused local anomalies in the bottom contours such that they were not quite straight and parallel. In particular, following a dredging event, the nearshore contours move landward more than the seaward contours. It is believed that this is an expression of the concentration of the longshore sediment transport in the nearshore zone.

The shoreline orientation was established by plotting and overlaying profiles located in the vicinity of the wave gages. The relative landward-seaward locations of the profiles were adjusted in the overlays to obtain best agreement by eye and the associated orientation determined. A range of orientations was obtained by matching the nearshore and offshore portions of the profiles. These ranges were qualitatively consistent with those determined from aerial photography, with the larger angles associated with the more seaward portions of the profiles.

TABLE III

SHORELINE ORIENTATION AS DETERMINED FROM BEACH AND OFFSHORE PROFILES

Date of Survey	Range of Effective Shoreline Orientation Relative to Baseline
May 8, 1974	9.95° to 11.33°
June 18, 1974	8.83° to 10.78°
Value Adopted In This Study	10.07°

Correlation of I with $P_{\ell s}$ and S_{xy}

In the correlation of $P_{\ell s}$ and S_{xy} with I, only the values directed toward the trap were used. The rationale is that during all periods when waves were directed toward the trap, there was sediment available for transport and therefore this variable provides the best basis for correlation.

The volumetric accumulations were interpreted as I values by Eq. (3) using p = 0.35 and by dividing by the time (in seconds) between surveys. The wave data were available nominally every two hours. The value of $P_{\ell s}$ (and S_{xy}) for a survey period was obtained by summing all $P_{\ell s}$ values directed toward the trap and dividing by the total number of wave recordings.

RESULTS

Table IV presents a summary of the analyzed data. A number of correlations were carried out to determine best fits of the transport data, I, with $P_{\ell s}$ and S_{xy}. These results are summarized in Table V.

TABLE IV

SUMMARY OF ANALYZED DATA

Survey Period	I (N/s)	$P_{\ell s_-}$ (N/s)	$P_{\ell s_+}$ (N/s)	S_{xy_-} (N/m)	S_{xy_+} (N/m)
July 30, 1974 to Aug. 20, 1974	182.1	120.3	49.9	22.3	10.3
Aug. 20, 1974 to Sept. 24, 1974	144.6	153.5	46.2	26.4	8.6
Sept. 24, 1974 to Nov. 6, 1974	171.2	295.8	158.2	39.2	25.6
Nov. 6, 1974 to Jan. 7, 1975	439.3	426.8	80.9	57.7	10.7
Jan. 7, 1975 to Feb. 11, 1975	401.4	446.6	0.0	57.0	0.2
Feb. 11, 1975 to March 4, 1975	245.8	330.9	144.5	45.7	17.5
March 4, 1975 to April 14, 1975	326.2	783.8	30.0	100.0	6.9

Note: $P_{\ell s_-}$ and S_{xy_-} represent fluxes toward the trap and $P_{\ell s_+}$ and S_{xy_+} represent fluxes away from the trap.

TABLE V

SUMMARY OF CORRELATIONS OF I WITH $P_{\ell s}$ AND S_{xy}

($P_{\ell s}$ and S_{xy} Are Values Directed Toward Trap)

Basis for Correlation	Coefficient	Percentage Standard Deviation in K or K_*
Least Squares Fit, Arithmetic Basis, $I = KP_{\ell s}$	$K = 0.65$	
Least Squares Fit, Logarithmic Basis, $I = KP_{\ell s}$	$K = 0.92$	
Individual Points $I = KP_{\ell s}$	$\bar{K} = 0.87$	39.6%
Least Squares Fit, Arithmetic Basis, $I = K_* S_{xy}$	$K_* = 4.98$ (m/s)	
Least Squares Fit, Logarithmic Basis, $I = K_* S_{xy}$	$K_* = 6.37$ (m/s)	
Individual Points $I = K_* S_{xy}$	$\bar{K}_* = 5.90$ (m/s)	33.3%

Figure 6 presents a plot of the seven data points in the form of I vs. $P_{\ell s}$ where the energy flux value is directed toward the trap. In addition, a sensitivity analysis has been performed in which the horizontal bars represent the variation in $P_{\ell s}$ due to a ±0.5° variation in orientation of the offshore pressure gages. The vertical bars represent the variation in I due to a uniform variation in sand elevation of ±5 cm over the area surveyed. The different bar lengths occur in $P_{\ell s}$ due to various effective wave approach angles and in I due to various volumes accumulated between surveys. It appears from Figure 6 that there is a low energy flux upward bias due to the tendency of the trap to collect material even for waves propagating directly toward shore.

SUMMARY AND CONCLUSIONS

Measurements of immersed sediment transport rate, I, as inferred from sediment accumulation in a near-total trap were correlated with longshore energy flux at breaking, $P_{\ell s}$, and the onshore flux of the longshore component of momentum, S_{xy}, as calculated from two pressure sensors mounted near the bottom.

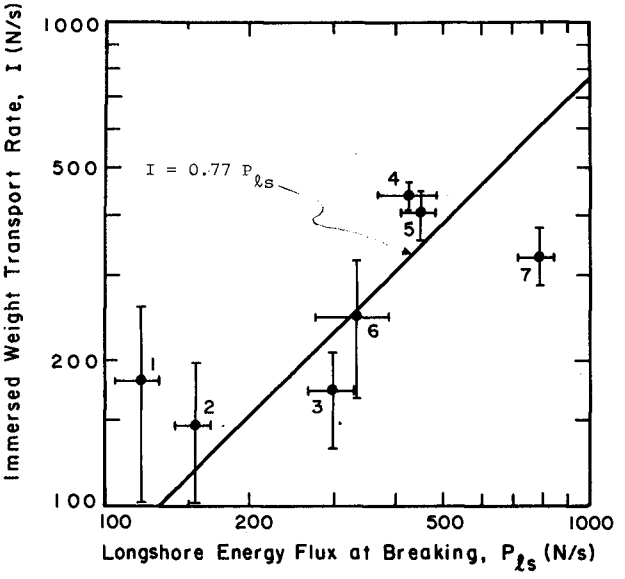

Figure 6. Plot of I vs. $P_{\ell s}$ Results From Present Study. Horizontal Bars Represent ±0.5° in Offshore Gage Orientation. Vertical Bars Represent ±5 cm Uniform Thickness of Sand. The Numbers Denote the Sequence of Intersurvey Periods.

Based on the analysis of seven volumetric accumulation periods, it is concluded that:

(1) On an overall basis, the results agree reasonably well with some of the previous studies. Depending on the method of analysis, the best fit dimensionless constant K in the relationship $I = KP_{\ell s}$ ranges from 0.65 to 0.92,

(2) For the same seven intersurvey periods, the K values obtained here are substantially lower than those obtained by Bruno and Gable (1976) as based on visual wave estimates. Their average K value is 1.40 as compared to 0.87 obtained here.

(3) A pair of wave gages appears to perform reasonably well to determine overall directional characteristics such as $P_{\ell s}$; however, the quality of the detailed directional results could be improved substantially by a greater number of gages.

(4) In calculating wave direction from an array of gages, it is extremely important to determine accurately the relative locations of the gages and the shoreline orientation. For

the present data, an angular misalignment of ±0.5° can cause an associated change in $P_{\ell s}$ ranging from 8% to 18%. This effect is accentuated for small obliquity of the incident waves.

(5) An offshore breakwater, if dredged below the equilibrium topography is expected to cause an upward bias in the volumes trapped. This effect appears present in the data; the points associated with small longshore energy flux values lie above the usual relationship. Moreover, there is a tendency for the individual K values to decrease as the trap fills (Figure 6). Unfortunately, at present, the magnitude of the bias exerted by an offshore breakwater on trapped quantities and the variation of this bias following a dredging event is unquantified. The best approach in the present case may be through the use of a detailed numerical model. It is expected that the K results developed in the present study contain an upward bias.

(6) There are variations in the K values that cannot be explained through appeal to any evident mechanisms or processes. For example, the K value associated with the last (seventh) intersurvey period is approximately one-half the average of the values for the fourth and fifth intersurvey periods.

(7) The environmental and economic significance of an improved quantitative predictor for longshore sediment transport justifies substantial future field programs to discern the effects of individual variables (e.g. grain size, beach slope, etc.) and in general, to develop a more accurate predictor.

ACKNOWLEDGEMENTS

The approval of the Coastal Engineering Research Center (CERC) to utilize the data forming the basis for this paper is appreciated. Dr. T. L. Walton of CERC offered helpful discussions and encouragement throughout the study. The Computing Center of the University of Delaware provided support for the required computer time.

REFERENCES

Bruno, R. O. and C. G. Gable, "Longshore Transport at a Total Littoral Barrier," Proceedings, Fifteenth International Conference on Coastal Engineering, Chapter 71, p. 1203-1222, 1976.

Bruno, R. O., Watts, G. M. and C. G. Gable, "Sediments Impounded by an Offshore Breakwater," Proceedings, ASCE Specialty Conference, Coastal Sediments '77, Charleston, SC, p. 1006-1025, 1977.

Caldwell, J. W., "Wave Action and Sand Movement Near Anaheim Bay, California," U. S. Army Beach Erosion Board Technical Memorandum No. 68, 1956.

Das, M. M., "Longshore Sediment Transport Rates: A Compilation of Data," U. S. Army Coastal Engineering Research Center Miscellaneous Paper No. 1-71, September, 1971.

Das, M. M., "Suspended Sediment and Longshore Sediment Transport Review," Chapter 54, Proceedings, Thirteenth Conference on Coastal Engineering, p. 1027-1048, 1972.

Galvin, C. J., "Comparison of Johnson's Littoral Drift Data for Santa Barbara with the Empirical Relation of CERC TR 4," Memorandum for Record, Coastal Engineering Research Center, February 1969.

Greer, M. N. and O. S. Madsen, "Longshore Sediment Transport Data: A Review," Chapter 93, Proceedings, Sixteenth Conference on Coastal Engineering, p. 1563-1576, 1978.

Harris, F. J., "Windows, Harmonic Analysis, and the Discrete Fourier Transform," Report NUC TP 532, Naval Undersea Center, San Diego, CA, September 1976.

Herron, W. J. and R. L. Harris, "Littoral Bypassing and Beach Restoration in the Vicinity of Port Hueneme, California," Proceedings, Tenth Conference on Coastal Engineering, ASCE, Chapter 38, pp. 651-675, 1966.

Inman, D. L. and R. A. Bagnold, "Littoral Processes," in The Sea, Edited by M. N. Hill, Volume 3, Interscience, p. 529-533, 1963.

Johnson, J. W., "Sand Transport by Littoral Currents," Institute of Engineering Research, Wave Research Laboratory, University of California at Berkeley, Technical Report Series 3, Issue 338, 1952.

Komar, P. D. and D. L. Inman, "Longshore Sand Transport on Beaches," J. Geophys. Res., Volume 75, No. 30, p. 5914-5927, October 20, 1970.

Komar, P. D., "The Mechanics of Sand Transport on Beaches," J. of Geophys. Res., Volume 76, No. 3, p. 713-721, January 20, 1971.

Moore, G. W. and J. Y. Cole, "Coastal Processes in the Vicinity of Cape Thompson, Alaska; Geologic Investigations in Support of Project Chariot in the Vicinity of Cape Thompson, Northwestern Alaska - Preliminary Report," U. S. Geological Survey Trace Elements Investigations Report 753, 1960.

Thornton, E. B., "Longshore Currents and Sediment Transport," Department of Coastal and Oceanographic Engineering, University of Florida, Technical Report No. 5, 1969.

U. S. Army Corps of Engineers, Coastal Engineering Research Center, "Shore Protection, Planning and Design, Technical Report No. 4," 1966.

U. S. Army Corps of Engineers, Coastal Engineering Research Center, "Volume I, Shore Protection Manual," U. S. Government Printing Office, 1973.

Watts, G. M., "A Study of Sand Movement at South Lake Worth Inlet, Florida," U. S. Army Beach Erosion Board Technical Memorandum No. 42, 1953.